Vol. 40 — N° 1 03 16 P. 5 – 27

GEOSTANDARDS and GEOANALYTICAL RESEARCH

A Flux-Free Fusion Technique for Rapid Determination of Major and Trace Elements in Silicate Rocks by LA-ICP-MS

Zhiwei **He** (1), Fang **Huang** (1)*, Huimin **Yu** (1), Yilin **Xiao** (1), Fangyue **Wang** (1, 2), Qiuli **Li** (3), Ying **Xia** (1) and Xingchao **Zhang** (1)

(1) Key Laboratory of Crust-Mantle Materials and Environments, School of Earth and Space Sciences, University of Science and Technology of China, Hefei, 230026, China
(2) School of Resources and Environmental Engineering, Hefei University of Technology, Hefei, 230009, China
(3) State Key Laboratory of Lithospheric Evolution, Institute of Geology and Geophysics, Chinese Academy of Sciences, Beijing, 100029, China
* Corresponding author. e-mail: fhuang@ustc.edu.cn

A simple flux-free fusion technique was developed to analyse major and trace element compositions of silicate rocks. The sample powders were melted in a molybdenum capsule sealed in a graphite tube to make a homogenous glass in a temperature-controlled one-atmosphere furnace. The glass was then measured for both major and trace element concentrations by LA-ICP-MS using a calibration strategy of total metal-oxide normalisation. The optimum conditions (i.e., temperature and duration) to make homogeneous glasses were obtained by performing melting experiments using a series of USGS reference materials including BCR-2, BIR-1, BHVO-2, AGV-1, AGV-2, RGM-1, W-2 and GSP-2 with SiO_2 contents from 47 to 73% *m/m*. Analytical results of the USGS reference materials using our method were generally consistent with the recommended values within a discrepancy of 5–10% for most elements. The routine precision of our method was generally better than 5–10% RSD. Compared with previous methods of LA-ICP-MS whole-rock analyses, our flux-free fusion method is convenient and efficient in making silicate powder into homogeneous glass. Furthermore, it limits contamination and loss of volatile elements during heating. Therefore, our new method has great potential to provide reliable and rapid determinations of major and trace element compositions for silicate rocks.

Keywords: LA-ICP-MS, bulk analysis, flux-free fusion, silicate rocks, molybdenum–graphite capsule.

Une technique simple de fusion sans flux a été développée pour analyser les compositions en éléments majeurs et traces de roches silicatées. Les poudres d'échantillons ont été fondues dans une capsule de molybdène scellée dans un tube de graphite pour la production d'un verre homogène dans un four à une atmosphère et température contrôlée. Le verre a ensuite été mesuré pour les concentrations en éléments majeurs et traces par LA-ICP-MS en utilisant une stratégie de calibration basée sur la normalisation totale des oxydes de métaux. Les conditions optimales (i.e, température et durée) pour faire des verres homogènes ont été obtenues en effectuant des expériences de fusion en utilisant une série de matériaux de référence USGS comprenant BCR-2, BIR-1, BHVO-2, AGV-1, AGV-2, RGM-1, W-2 GSP-2 avec un contenu en SiO_2 compris entre 47 et 73% m/m. Les résultats de l'analyse des matériaux de référence USGS en utilisant notre méthode sont généralement compatibles avec les valeurs recommandées dans un intervalle de 5 à 10% pour la plupart des éléments. La précision de routine de notre méthode est généralement meilleure que 5–10% RSD. Par rapport aux méthodes précédentes d'analyse sur roche totale par LA-ICP-MS, notre méthode de fusion sans flux est pratique et efficace par la production de verres homogènes à partir de poudres de silicate. En outre, elle limite la contamination et la perte d'éléments volatils pendant le chauffage. Par conséquent, notre nouvelle méthode a un grand potentiel pour fournir des déterminations fiables et rapides des compositions en éléments majeurs et traces des roches silicatées.

Mots-clés : LA-ICP-MS, analyse roche totale, fusion sans flux, roches silicatées, capsule molybdène-graphite.

Received 29 Nov 14 – Accepted 20 Feb 15

doi: 10.1111/j.1751-908X.2015.00352.x

Determination of the elemental composition of silicate rocks provides essential information about their geochemical characteristics. Solution ICP-MS analysis of samples treated by wet chemistry digestion or alkali fusion is a conventional method for multi-element determinations that is time-consuming and complicated (e.g., Jarvis 1988, Jenner *et al.* 1990, Eggins *et al.* 1997, Yu *et al.* 2001, Awaji *et al.* 2006, Pretorius *et al.* 2006, Bayon *et al.* 2009, Park *et al.* 2013). In contrast, laser ablation ICP-MS (LA-ICP-MS) has advantages in several respects, including quick sample preparation, *in situ* analysis and low blank levels. It has become a powerful tool for rapid and precise determination of chemical compositions in geological and environmental samples (e.g., Fedorowich *et al.* 1993, Jarvis and Williams 1993, Perkins *et al.* 1993, Gao *et al.* 2002, Stoll *et al.* 2008, Hu *et al.* 2009, Chen *et al.* 2011, Li *et al.* 2011, Jochum *et al.* 2012, Malherbe *et al.* 2013, Nielsen and Lee 2013, Zhu *et al.* 2013, Mukherjee *et al.* 2014).

The sample preparation processes are critical for LA-ICP-MS analysis of whole-rock powdered samples. Commonly used preparation techniques include the use of (a) pressed powder pellets, (b) flux-addition fusion and (c) flux-free fusion.

The pressed powder pellet technique has been widely applied to igneous rocks and soil samples (e.g., Gray 1985, Van Heuzen and Morsink 1991, Pearce *et al.* 1992, Jarvis and Williams 1993, Lee *et al.* 2003, Mukherjee *et al.* 2014). The powdered samples are usually spiked with internal standard elements or enriched isotopes and then pressed into a pellet for LA-ICP-MS analysis (Lee *et al.* 2003). However, the analytical precision of this method is not high enough (about 10–20% RSD) compared with solution ICP-MS and other bulk analysis techniques (Stoll *et al.* 2008). Several factors (such as the sample grain size, pellet compactness and amount of binding media) can potentially affect the homogeneity of the pellets, resulting in significant analytical uncertainties (Mukherjee *et al.* 2014).

The flux-addition fusion technique can produce homogeneous glasses by mixing a flux agent (e.g., lithium borate) with sample powders. However, because of the dilution of the lithium borate flux, this technique increases the detection limits of trace elements, hampering accurate analysis for low-abundance elements (Eggins 2003, Yu *et al.* 2003). Additionally, the ICP-MS can be contaminated by 'sticky' elements (such as Li, B and Cs) from the flux (Sylvester 2001).

In contrast, the flux-free fusion method can directly melt sample powders into homogenous glasses without adding fluxes or standard elements. Previous studies have developed different methods to make silicate glasses by using the following: (1) special metal (e.g., W, Ir and Mo) strip heaters (Nicholls 1974, Brown 1977, Fedorowich *et al.* 1993, Reid *et al.* 1999, Nehring *et al.* 2008, Stoll *et al.* 2008); (2) welded platinum capsules (Kurosawa *et al.* 2006); and (3) boron nitride (BN) hermetic crucibles (Zhu *et al.* 2013). Although these techniques are rapid and simple, some problems remain. For example, the use of metal strip heaters could cause depletion of volatile elements (e.g., Cs, Pb and Zn) because of the high melting temperature (> 1600 °C) required for making the glasses. In addition, using welded platinum capsules may cause loss of transition metals into the platinum capsule during melting (Kurosawa *et al.* 2006); platinum is also expensive. Boron nitride is so reducing that transition metals (such as Cr, Ni and Cu) may precipitate from the melt (Zhu *et al.* 2013).

In this study, in order to minimise the drawbacks of sample preparation methods, we established a new flux-free fusion method for routine LA-ICP-MS whole-rock analyses. Briefly, we used a molybdenum (Mo) capsule sealed in a graphite tube (Figure 1) to make silicate glasses in a temperature-controlled one-atmosphere furnace. Following this, both major and trace element contents of the glasses were determined simultaneously by LA-ICP-MS. Homogeneity of the fused glasses and accuracy of LA-ICP-MS data were rigorously evaluated to prove the reliability of this method.

Experiments

Reference materials and samples

The USGS reference materials used in this study included three basalts (BIR-1, BHVO-2 and BCR-2), two andesites (AGV-1 and AGV-2), one rhyolite (RGM-1), one diabase (W-2) and one granodiorite (GSP-2). We also analysed two well-characterised natural samples (basalt 13AFS-2 and granodiorite 06TG-1). The RMs and natural samples display a wide range of SiO_2 contents from 44% to 73% *m/m*. The recommended values of major and trace element contents for BIR-1, BHVO-2, BCR-2, AGV-1, AGV-2 and W-2 were taken from the GeoReM database (http://georem.mpch-mainz.gwdg.de/). The reference values for RGM-1 were taken from the GeoReM database, which were cited by Zhu *et al.* (2013). The reference values for GSP-2 were from Wilson (1998) and Cotta and Enzweiler (2012). The reference major and trace element contents of basalt 13AFS-2 were derived from XRF spectrometry and solution ICP-MS, respectively (J. Huang, S.G. Li, Y.L. Xiao, S. Ke, W.Y. Li, Y. Tian, unpublished data). The reference data of granodi-

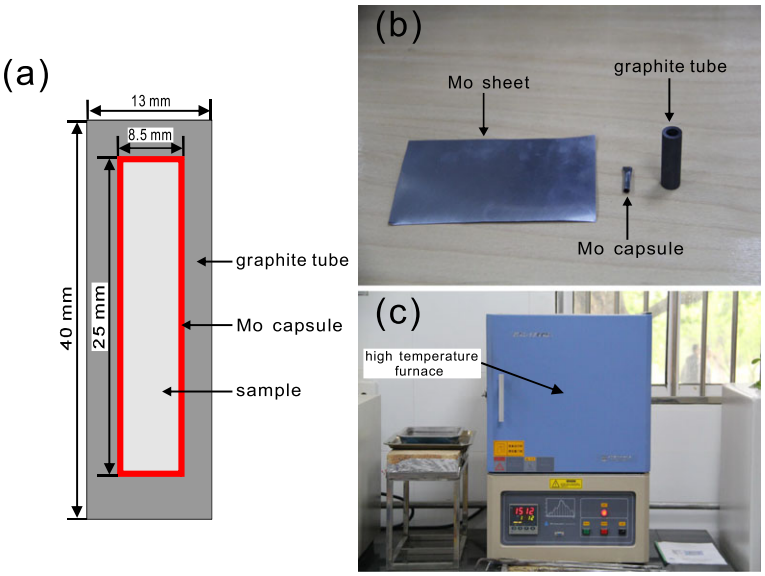

Figure 1. (a) Cross section of the Mo–graphite assembly used for flux-free fusion in our study. (b) Parts to make the Mo–graphite assembly, including molybdenum sheet, capsule made of Mo sheet and graphite tube. (c) Overview of the one-atmosphere furnace in the laboratory at the USTC.

orite 06TG-1 were measured by XRF spectrometry and LA-ICP-MS with $LiBO_3$ fusion (He *et al.* 2011).

Sample preparation procedure

The success of the flux-free fusion method hinges on whether silicate rock powders can be efficiently fused into homogenous glasses. We used a graphite–Mo assembly to do so, illustrated in Figure 1a. A Mo sheet (0.2 mm thick; purity = 99.9%) was cut into rectangular fragments (27 mm long and 25 mm wide), which were then rolled into capsules (Figure 1b). To avoid any contamination of the surface of the Mo sheet, the Mo capsules were cleaned for 10 min in an ultrasonic bath with 5% *v/v* HNO_3 and then dried before being filled with test portion powder. About 0.3 g of powder was put in the cleaned Mo capsule using a stainless steel scoop. Finally, the capsule was placed in the graphite tube.

Melting experiments were performed in a high-temperature one-atmosphere furnace (KSL-1700X-A4) produced by the Hefei Kejing Material Technology Company (Figure 1c). The volume of the oven chamber was 36 litres (30 cm × 40 cm × 30 cm), allowing at least ten samples to be melted simultaneously. The melting conditions were controlled by an intelligent programmable system with a heating rate of 10 °C min^{-1}. The highest temperature designed for the furnace is 1700 °C, while the routine working temperature was less than 1650 °C.

After heating to fusion in the furnace at high temperature for a given duration, the sample-contained graphite–Mo assemblies were quenched to room temperature within a few seconds by dropping them into cool water. The quenched glasses were then removed from the capsules, mounted in petro-epoxy, and well polished for microscopic observation and LA-ICP-MS analyses.

Instrumentation

LA-ICP-MS analyses in our study were mainly performed at the Chinese Academy of Sciences Key Laboratory of Crust-Mantle Materials and Environments, University of Science and Technology of China (USTC), Hefei, China. For a comparison, a fused AGV-2 glass (1400 °C, 10 min) was also measured at the State Key Laboratory of Geological Processes and Mineral Resources, China University of Geosciences (CUG), Wuhan, China.

In the USTC laboratory, an Agilent 7700e ICP-MS was combined with a GeolasPro ArF (193 nm) excimer laser sampling system. The fused glasses were ablated in single-spot mode, with a spot size of 44 μm and repetition rate of 10 Hz. Helium was used as the carrier gas flowing through the sample cell, with the aerosol materials ablated by laser into the ICP-MS. Argon was used as the make-up gas to mix with He before entering the plasma. The instrumental operating parameters (e.g., carrier gas, make-up gas flows and sampling depth) were optimised by ablating NIST SRM

610 to obtain the strongest signal intensity for ^{208}Pb while keeping ThO^+/Th^+ (1.5–2%) and Ca^{2+}/Ca^+ (~ 0.2%) low, to minimise the interferences from oxide and doubly charged ions. The Th^+/U^+ ratio was close to 1 when ablating NIST SRM 610, indicating a high ionisation rate of the laser-generated particles (Guillong and Günther 2002, Günther and Hattendorf 2005).

The detailed LA-ICP-MS instrumental operation conditions are listed in Table 1. During each LA-ICP-MS analysis, it took about 25 s for blank, 40 s for ablation and 35 s for gas flow washing. All data acquisition occurred in time-resolved analysis mode. In the CUG laboratory, major and trace elements were determined using an Agilent 7500a ICP-MS in combination with an excimer 193-nm laser ablation system (GeoLas 2005). Single-spot mode with spot size of 44 μm was applied, and the other operating conditions were same as those described by Liu *et al.* (2008).

Data processing

In this study, we applied the calibration strategy of summed metal-oxide normalisation for data reduction. Briefly, the sum of all measured metal oxides was normalised to 100% *m/m* after subtracting the loss on ignition (Halicz and Günther 2004, Guillong *et al.* 2005, Liu *et al.* 2008, Zhu *et al.* 2013). Compared with calibration combined with internal standardisation, this method can obtain major and trace element contents simultaneously without an internal standard element predetermined by electron probe micro-analysis (EPMA) or XRF spectrometry. Three USGS basalt glass reference materials (BHVO-2G, BCR-2G and BIR-1G) were used for calibration, which can provide more precise and accurate elemental concentrations relative to calibration using NIST SRM 610 (Liu *et al.* 2008). The anticipated measurement uncertainties of this calibration method are generally within 5% for major elements (RSD = 0.3–3.9% except for P_2O_5), and 5–10% for trace elements based on analyses of MPI-DING reference glasses (Liu *et al.* 2008). The sequence of analysis began with four analyses of reference glasses (NIST SRM 610, BHVO-2G, BCR-2G and BIR-1G), followed by analyses of samples and then four analyses of reference glasses again. NIST SRM 610 was repetitively analysed every eight sample analyses for time-drift correction. ICPMSDataCal software (copyright reserved by Wuhan Sample Solution Analytical Technology Co., Ltd., Wuhan, China) edited by Liu *et al.* (2008) was used to perform the offline selection and integration of background and ablation signals, time-drift correction and quantitative calibration. Measurement uncertainties due to various oxidation states of Fe and Mn, matrix interferences, and trace metal elements and anions (e.g., F, Cl and OH) that were not analysed were discussed in detail by Liu *et al.* (2008).

Table 1.
Summary of the operating conditions for LA-ICP-MS analysis in this study

ICP-MS (Agilent 7700e)	
RF power	1350 W
Plasma gas	14 l min^{-1} Ar
Auxiliary gas	0.9 l min^{-1} Ar
Make-up gas	0.75 l min^{-1} Ar
Sampling depth	7.0 mm
Sample cone	1 mm Ni
Skimmer cone	0.4 mm Ni
Dwell time	5 ms for major elements; 10 ms for trace elements
Detector	Dual (pulse and analogue counting)
Laser (GeolasPro)	
Wavelength	193 nm
Energy density	10 J cm^{-2}
Carrier gas	0.6 l min^{-1} He
Ablation style	Single spot
Laser pulse	400
Ablation spot size	44 μm
Repetition rate	10 Hz

Results and discussion

Optimum melting conditions for extrusive rocks

For the flux-free fusion technique, melting temperature and duration are the most critical parameters to make homogenous glasses. Melting at optimum conditions should dissolve all refractory minerals and avoid significant loss of volatile elements (such as Cs, Pb and Zn) (Stoll *et al.* 2008). Relative to intrusive rocks, extrusive rocks are more easily fully fused because they contain smaller amounts of refractory minerals and the mineral sizes are also smaller. In our study, basalt and andesite RMs, BCR-2 and AGV-2, were selected to assess the effect of melting conditions on element homogeneity and analytical accuracy of fused glasses for extrusive rocks.

We first obtained AGV-2 glass fused at 1400 °C for 10 min, and then BCR-2 and AGV-2 glasses at 1450 °C for 5, 10 and 15 min, respectively. As shown in Figure 2a, b, both BCR-2 and AGV-2 glasses contained numerous vapour bubbles, while a significant amount of pure glass was also preserved. To eliminate the effect of bubbles on sample analysis, random spots on the bubble-free solid glass zones were targeted for LA-ICP-MS analysis. No metal grains or residual refractory minerals within the glass beads were observed using scanning electron microscopy, indicating homogeneity of the BCR-2 and AGV-2 glasses.

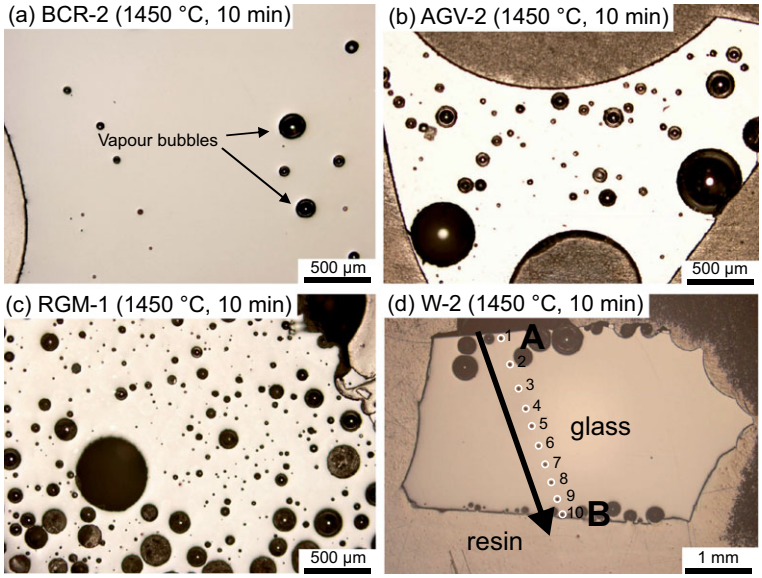

Figure 2. Photomicrographs of polished glass beads of (a) BCR-2, (b) AGV-2 and (c) RGM-1, respectively. The vapour bubbles are shown in the glass beads. (d) Ten laser spots (44 µm) along the A–B profile in the W-2 glass bead.

LA-ICP-MS analyses further confirmed that most elements were homogenously distributed in both AGV-2 and BCR-2 glasses at a spot scale of 44 µm. Table 2 summarises the LA-ICP-MS data from AGV-2 and BCR-2 glasses fused under different conditions. RSD values are used to evaluate the homogeneity of element distribution in these glasses. In order to address measurement reproducibility, we performed multi-spot analyses on different pieces of glass beads instead of multiple analyses of the same bead. Figure 3a shows that AGV-2 glass produced at 1400 °C for 10 min generally gave higher RSD values for most elements than that made at 1450 °C for 10 min, indicating that elevating the melting temperature could effectively homogenise the melt. In contrast, RSD values were generally lower than 10% and only changed slightly for most elements when fused at 1450 °C for 5, 10 and 15 min (Figure 3a). Such a phenomenon is also illustrated in Figure 4a. This implies that changing fusion duration from 5 min to 15 min did not obviously improve the glass homogeneity for most elements.

Notably, some elements (mainly Cr, Co, Ni, Zn and Pb) showed relative high RSD values (> 10%) in the BCR-2 glass fused at 1450 °C for 15 min relative to that fused for 5–10 min (Figure 4a). This may be attributed to reactions between the melt and the Mo capsule or contamination of Cr, Co and Ni during prolonged fusion process. The high RSD values (> 10%) for Zn and Pb may have been caused by volatilisation, indicating that prolonged fusion durations do not always ensure better homogeneity of elements such as Cr, Co, Ni, Zn and Pb. Therefore, a moderate melting condition (1450 °C, 10 min) may be more appropriate for melting basaltic and andesitic extrusive rocks.

The accuracy of the LA-ICP-MS data was evaluated by comparing the results with recommended values from the GeoReM database. Figures 3b and 4b show that analytical data for BCR-2 and AGV-2 glasses produced at different melting conditions (1400–1450 °C, 5–15 min) generally agree with the recommended values within 5–10% for most elements. To minimise possible contamination or volatilisation during prolonged melting, we selected 1450 °C and 10 min as the routine melting conditions for extrusive rocks.

Noticeable discrepancies were observed for Ni and Cu in the BCR-2 glass (e.g., Ni: 11.5 µg g^{-1}; Cu: 17 µg g^{-1} of glass fused at 1450 °C for 10 min) compared with the preferred values from the GeoReM database (Ni: 18 ± 1 µg g^{-1}; Cu: 21 ± 1 µg g^{-1}), but the results were in good agreement with recently published data (Ni: 11.8–13.9 µg g^{-1}; Cu: 16.6–18.0 µg g^{-1}) (Stoll *et al.* 2008, Cotta and Enzweiler 2012, Zhang *et al.* 2012). It was suggested that more analyses would be helpful to better constrain the Ni and Cu contents of BCR-2 given the limited number of sample analyses (Zhang *et al.* 2012, Hu *et al.* 2013).

Optimum melting conditions for granitoids

In contrast to extrusive rocks, granitoids are difficult to completely fuse due to the high viscosity of the melt and

GEOSTANDARDS and GEOANALYTICAL RESEARCH

Table 2.
Results for forty-five major and trace elements in AGV-2 and BCR-2 glasses fused at different melting conditions

Sample name			AGV-2									
Element	Isotope	Unit	Ref. value		1400 °C, 10 min		1450 °C, 5 min		1450 °C, 10 min		1450 °C, 15 min	
			Conc.	1*s*	Ave., *n* = 28	1*s*	Ave., *n* = 5	1*s*	Ave., *n* = 10	1*s*	Ave., *n* = 5	1*s*
SiO_2	29	% *m/m*	59.3	0.7	60.6	0.7	60.3	0.5	60.0	0.3	59.5	0.2
TiO_2	48	% *m/m*	1.05	0.22	1.00	0.07	0.94	0.06	1.00	0.08	0.99	0.002
Al_2O_3	27	% *m/m*	16.91	0.21	17.2	0.3	17.9	0.3	17.8	0.3	17.6	0.2
FeO (total)	57	% *m/m*	6.02	0.12	6.17	0.35	5.96	0.16	6.18	0.20	6.61	0.05
MnO	55	% *m/m*	0.1	0.004	0.10	0.01	0.10	0.01	0.10	0.00	0.10	0.002
MgO	25	% *m/m*	1.79	0.03	1.62	0.08	1.74	0.04	1.78	0.03	1.76	0.02
CaO	43	% *m/m*	5.2	0.13	5.13	0.19	5.15	0.13	5.24	0.23	5.32	0.07
Na_2O	23	% *m/m*	4.19	0.13	4.40	0.08	4.34	0.02	4.24	0.08	4.46	0.03
K_2O	39	% *m/m*	2.88	0.11	2.93	0.08	2.74	0.05	2.85	0.10	2.81	0.01
P_2O_5	31	% *m/m*	0.48	0.02	0.50	0.05	0.46	0.02	0.45	0.02	0.51	0.02
Li	7	$\mu g\ g^{-1}$	11	1	10.1	0.4	11.4	1.1	9.90	0.59	11.0	0.7
Sc	45	$\mu g\ g^{-1}$	13	1	13.1	0.7	12.7	0.3	13.0	0.9	12.6	0.3
V	51	$\mu g\ g^{-1}$	122	4	117	9	113	6	119	5	120	3
Cr	53	$\mu g\ g^{-1}$	16	1	15.6	3.1	15.6	3.7	18.0	1.6	15.2	1.8
Co	59	$\mu g\ g^{-1}$	16	1	14.2	2.5	15.5	1.4	14.7	0.4	15.3	0.5
Ni	60	$\mu g\ g^{-1}$	20	1	14.6	6.1	18.4	2.0	16.6	2.5	19.4	2.1
Cu	63	$\mu g\ g^{-1}$	53	4	49.4	3.9	51.3	0.8	48.4	1.5	50.8	1.1
Zn	66	$\mu g\ g^{-1}$	86	8	91.8	17.0	89.4	5.3	89.0	5.4	94.0	2.6
Ga	71	$\mu g\ g^{-1}$	20	1	21.4	2.7	19.6	0.5	20.8	1.0	21.1	0.7
Rb	85	$\mu g\ g^{-1}$	66.3	0.5	69.4	2.0	65.6	1.5	64.7	2.3	67.3	0.6
Sr	88	$\mu g\ g^{-1}$	661	6	650	22	681	15	678	5	687	5
Y	89	$\mu g\ g^{-1}$	19	2	18.6	1.1	19.4	0.9	19.2	0.6	19.8	0.5
Zr	91	$\mu g\ g^{-1}$	230	4	226	11	233	11	237	12	241	7
Nb	93	$\mu g\ g^{-1}$	14.5	0.8	14.4	0.9	14.0	0.9	14.6	0.7	14.9	0.7
Cs	133	$\mu g\ g^{-1}$	1.2	0.1	1.16	0.10	1.27	0.10	1.19	0.11	1.30	0.08
Ba	137	$\mu g\ g^{-1}$	1130	11	1133	29	1131	26	1134	30	1174	17
La	139	$\mu g\ g^{-1}$	37.9	0.04	36.5	1.7	37.8	1.4	37.6	1.5	38.8	0.4
Ce	140	$\mu g\ g^{-1}$	68.6	0.5	67.2	3.4	71.2	2.6	71.0	1.6	72.2	0.7
Pr	141	$\mu g\ g^{-1}$	7.84	0.31	7.72	0.43	7.99	0.31	8.17	0.2	8.11	0.09
Nd	143	$\mu g\ g^{-1}$	30.5	0.1	29.7	2.0	30.9	0.9	31.6	1.2	31.5	1.3
Sm	147	$\mu g\ g^{-1}$	5.49	0.03	5.61	0.63	5.78	0.53	5.60	0.32	6.36	0.27
Eu	151	$\mu g\ g^{-1}$	1.53	0.02	1.64	0.18	1.60	0.08	1.57	0.07	1.68	0.05
Gd	155	$\mu g\ g^{-1}$	4.52	0.05	4.37	0.49	5.04	0.43	5.16	0.29	5.21	0.14
Tb	159	$\mu g\ g^{-1}$	0.64	0.01	0.59	0.06	0.64	0.04	0.64	0.04	0.66	0.03
Dy	163	$\mu g\ g^{-1}$	3.47	0.03	3.45	0.32	3.50	0.15	3.61	0.28	3.58	0.07
Ho	165	$\mu g\ g^{-1}$	0.65	0.03	0.65	0.08	0.65	0.04	0.68	0.05	0.69	0.03

Table 2 (continued).
Results for forty-five major and trace elements in AGV-2 and BCR-2 glasses fused at different melting conditions

Sample name			AGV-2									
Element	Isotope	Unit	Ref. value		1400 °C, 10 min		1450 °C, 5 min		1450 °C, 10 min		1450 °C, 15 min	
			Conc.	1*s*	Ave., *n* = 28	1*s*	Ave., *n* = 5	1*s*	Ave., *n* = 10	1*s*	Ave., *n* = 5	1*s*
Er	166	μg g^{-1}	1.81	0.02	1.79	0.23	1.96	0.10	1.82	0.11	2.00	0.08
Tm	169	μg g^{-1}	0.26	0.01	0.25	0.03	0.25	0.02	0.25	0.02	0.25	0.03
Yb	173	μg g^{-1}	1.62	0.02	1.75	0.20	1.59	0.23	1.78	0.13	1.62	0.13
Lu	175	μg g^{-1}	0.247	0.004	0.25	0.05	0.25	0.02	0.25	0.02	0.26	0.02
Hf	178	μg g^{-1}	5	0.1	5.02	0.39	5.12	0.40	5.22	0.33	5.26	0.23
Ta	181	μg g^{-1}	0.87	0.08	0.84	0.07	0.81	0.06	0.88	0.07	0.86	0.08
Pb	208	μg g^{-1}	13.2	0.5	14.1	2.2	14.3	0.3	14.0	0.4	16.0	1.8
Th	232	μg g^{-1}	6.1	0.2	5.84	0.26	6.11	0.25	6.24	0.31	6.27	0.15
U	238	μg g^{-1}	1.86	0.09	1.81	0.13	1.92	0.08	1.80	0.08	1.93	0.07

Sample name			BCR-2							
Element	Isotope	Unit	Ref. value		1450 °C, 5 min		1450 °C, 10 min		1450 °C, 15 min	
			Conc.	1*s*	Ave. (*n* = 14)	1*s*	Ave. (*n* = 14)	1*s*	Ave. (*n* = 14)	1*s*
SiO_2	29	% *m/m*	54.1	0.8	54.1	0.8	53.4	0.4	53.6	0.5
TiO_2	48	% *m/m*	2.26	0.05	2.33	0.09	2.39	0.07	2.41	0.05
Al_2O_3	27	% *m/m*	13.5	0.2	13.9	0.1	14.2	0.1	14.2	0.1
FeO (total)	57	% *m/m*	12.42	0.18	12.8	0.3	12.9	0.4	12.6	0.27
MnO	55	% *m/m*	0.2	0.01	0.21	0.00	0.21	0.00	0.21	0.002
MgO	25	% *m/m*	3.59	0.05	3.56	0.05	3.62	0.06	3.63	0.05
CaO	43	% *m/m*	7.12	0.11	7.42	0.19	7.59	0.12	7.64	0.13
Na_2O	23	% *m/m*	3.16	0.11	3.24	0.06	3.28	0.08	3.27	0.03
K_2O	39	% *m/m*	1.79	0.05	1.76	0.04	1.76	0.03	1.78	0.04
P_2O_5	31	% *m/m*	0.35	0.02	0.35	0.01	0.36	0.01	0.36	0.02
Li	7	μg g^{-1}	9	2	8.89	0.39	8.91	0.46	8.93	0.29
Sc	45	μg g^{-1}	33	2	34.6	1.0	34.9	0.8	35.5	0.9
V	51	μg g^{-1}	416	14	429	12	436	11	446	6
Cr	53	μg g^{-1}	18	2	16.6	1.8	16.9	1.4	21.5	3.8
Co	59	μg g^{-1}	37	3	35.7	1.4	36.9	1.3	36.3	5.1
Ni	60	μg g^{-1}	18	1	9.89	1.50	11.5	1.0	9.48	2.19
Cu	63	μg g^{-1}	21	1	25.6	2.4	17.0	0.4	17.2	0.7
Zn	66	μg g^{-1}	127	9	135	14	133	3	114	18
Ga	71	μg g^{-1}	23	2	22.3	0.3	22.2	0.3	21.7	0.9
Rb	85	μg g^{-1}	46.9	0.1	46.1	1.0	46.5	1.3	47.0	1.0
Sr	88	μg g^{-1}	340	3	352	3	358	5	360	6
Y	89	μg g^{-1}	37	2	36.0	0.5	36.6	0.7	36.8	0.8

GEOSTANDARDS and GEOANALYTICAL RESEARCH

GEOSTANDARDS and GEOANALYTICAL RESEARCH

Table 2 (continued).
Results for forty-five major and trace elements in AGV-2 and BCR-2 glasses fused at different melting conditions

Sample name			BCR-2							
Element	Isotope	Unit	Ref. value		1450 °C, 5 min		1450 °C, 10 min		1450 °C, 15 min	
			Conc.	1*s*	Ave. (*n* = 14)	1*s*	Ave. (*n* = 14)	1*s*	Ave. (*n* = 14)	1*s*
Zr	91	μg g^{-1}	184	1	186	3	187	4	192	4
Nb	93	μg g^{-1}	12.6	0.4	12.7	0.2	13.0	0.3	13.1	0.2
Cs	133	μg g^{-1}	1.1	0.1	1.15	0.04	1.16	0.05	1.17	0.05
Ba	137	μg g^{-1}	677	2	689	7	700	8	705	12
La	139	μg g^{-1}	24.9	0.2	25.6	0.2	25.8	0.3	26.0	0.6
Ce	140	μg g^{-1}	52.9	0.2	54.2	0.5	54.3	1.0	54.7	1.1
Pr	141	μg g^{-1}	6.7	0.1	6.96	0.12	6.96	0.14	6.98	0.09
Nd	143	μg g^{-1}	28.7	0.1	29.8	0.8	29.9	0.8	29.7	1.0
Sm	147	μg g^{-1}	6.58	0.02	6.72	0.20	6.68	0.30	6.98	0.26
Eu	151	μg g^{-1}	1.96	0.01	2.04	0.09	2.09	0.05	2.10	0.08
Gd	155	μg g^{-1}	6.75	0.03	7.11	0.18	6.98	0.16	7.23	0.16
Tb	159	μg g^{-1}	1.07	0.03	1.07	0.04	1.05	0.03	1.07	0.04
Dy	163	μg g^{-1}	6.41	0.05	6.42	0.19	6.44	0.19	6.47	0.26
Ho	165	μg g^{-1}	1.28	0.03	1.30	0.04	1.30	0.05	1.30	0.04
Er	166	μg g^{-1}	3.66	0.01	3.82	0.14	3.76	0.13	3.80	0.10
Tm	169	μg g^{-1}	0.54	0.04	0.53	0.02	0.53	0.02	0.51	0.03
Yb	173	μg g^{-1}	3.38	0.02	3.37	0.12	3.41	0.10	3.42	0.16
Lu	175	μg g^{-1}	0.503	0.009	0.49	0.03	0.48	0.02	0.48	0.02
Hf	178	μg g^{-1}	4.9	0.1	4.91	0.25	4.84	0.18	4.92	0.10
Ta	181	μg g^{-1}	0.74	0.02	0.81	0.03	0.80	0.03	0.79	0.03
Pb	208	μg g^{-1}	11	1	11.4	0.4	11.1	0.6	8.41	1.32
Th	232	μg g^{-1}	5.7	0.5	5.93	0.14	5.88	0.20	5.91	0.08
U	238	μg g^{-1}	1.69	0.19	1.65	0.06	1.64	0.05	1.64	0.05

Ref. value, reference values for AGV-2 and BCR-2 were taken from the preferred values in the GeoReM database (http://georem.mpch-mainz.gwdg.de/); Conc., concentration; Ave., Average; *s*, standard deviation.

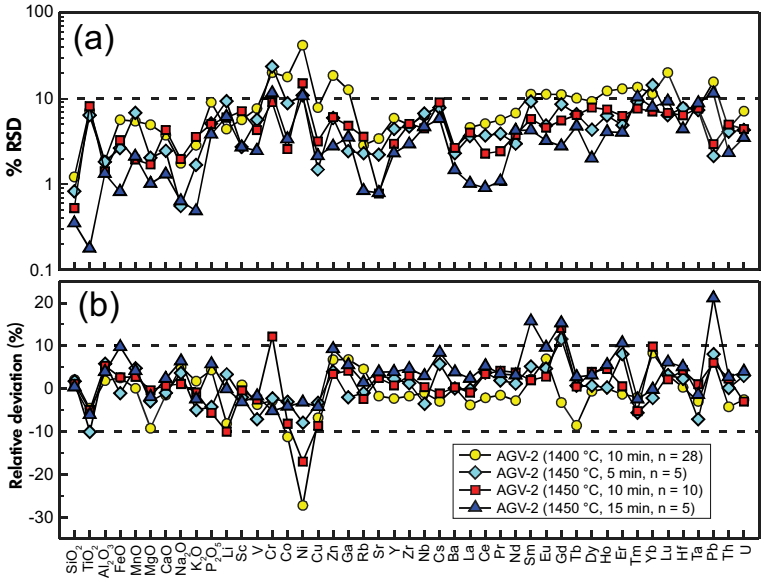

Figure 3. Effect of melting conditions (1400 °C, 10 min and 1450 °C, 5–15 min) on (a) relative standard deviations (RSD) and (b) relative deviations (RD) [100× (measured values - reference values)/reference values)] of the measured values from the reference values in the AGV-2 glasses.

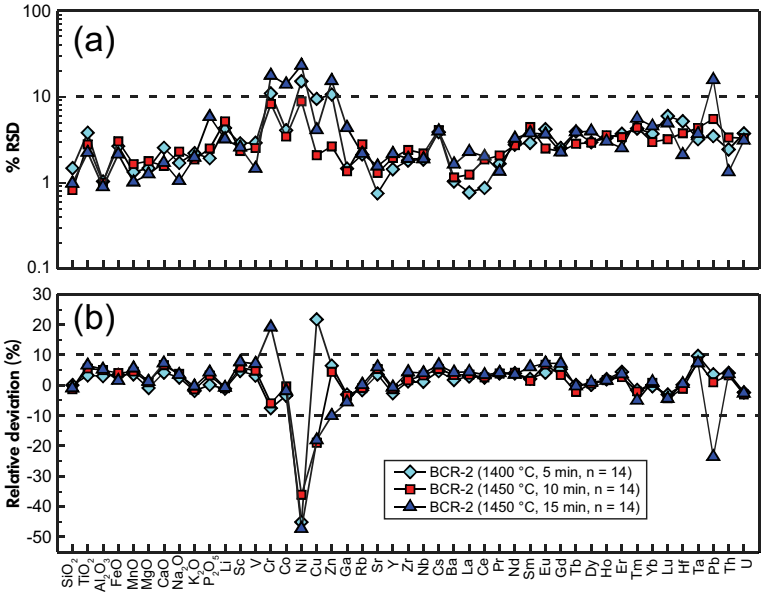

Figure 4. Effect of melting conditions (1450 °C and 5–15 min) on (a) RSD and (b) relative deviations of the measured values from the reference values in the BCR-2 glasses.

the low solubility of zircon in high-SiO_2 melts. This may cause significant heterogeneity for Zr, Hf and heavy rare earth elements (HREEs) due to their high compatibility in zircon. USGS granodiorite reference material GSP-2 (with a high Zr content of 550 μg g^{-1}) was selected to evaluate the effect of melting conditions on analytical performance for granitoids. Relative to volcanic rocks, higher temperatures (1550–1600 °C) and longer durations (25–35 min) were applied to GSP-2. Figure 5 shows that small amounts of residual zircons (10–20 μm) were preserved in the melt even under extreme fusion conditions, indicating complete decomposition of zircon is difficult for granitoids using the conventional flux-free fusion technique.

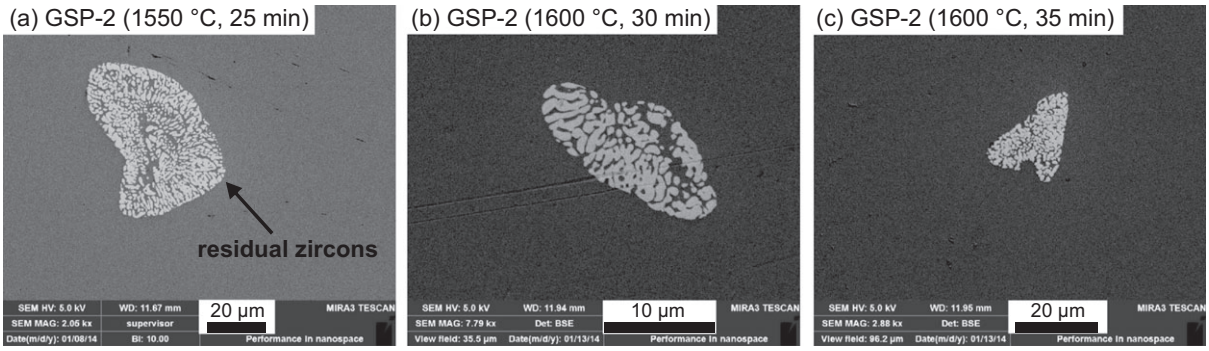

Figure 5. Back-scattered electron SEM images of residual zircons in GSP-2 glasses fused at (a) 1550 °C for 25 min, (b) 1600 °C for 30 min and (c) 1600 °C for 35 min.

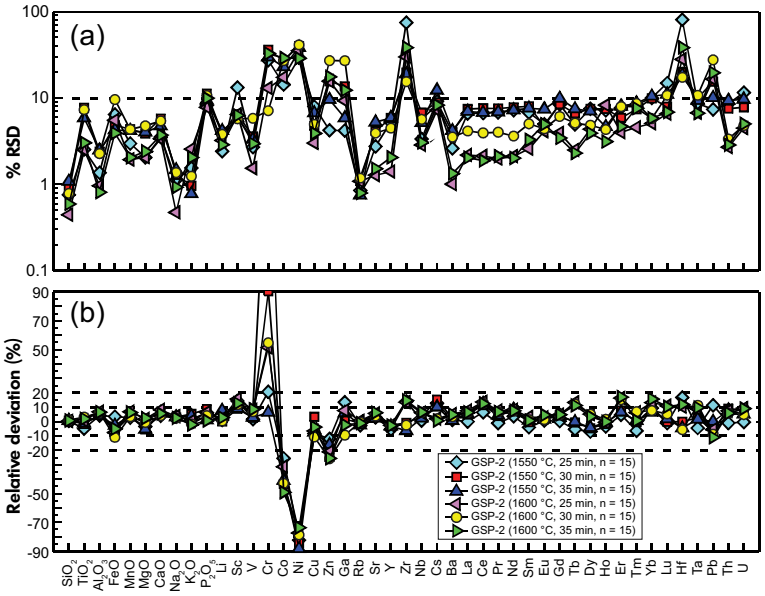

Figure 6. Effect of melting conditions (1550–1600 °C, 25–35 min) on (a) RSD and (b) relative deviations of the measured values from the reference values for the GSP-2 glasses.

Analytical results for GSP-2 glasses fused at different melting conditions are listed in Table 3. Figure 6a demonstrates the effects of different melting temperatures and durations on homogeneity of elements. It is clear that RSD values of GSP-2 glasses show similar distribution patterns even though melting temperature changed from 1550 °C to 1600 °C and durations from 25 to 35 min. Analytes including P_2O_5, Cr, Co and Ni were found to be heterogeneously distributed as displayed in their systematically high RSD values. Zirconium and Hf were also heterogeneous, with RSD values greater than 10–20%, confirming the influence of residual zircon grains. Our data illustrate that volatile elements (e.g., Zn, Ga, Cs and Pb) were generally homogeneously distributed (RSD < 10–20%). Notably, for elements that are not sensitive to volatilisation or crystallisation of refractory minerals (e.g., Na_2O, K_2O, Rb, Sr and light rare earth elements (LREEs)), RSD values were generally less than 5–10%.

The accuracy of LA-ICP-MS data for GSP-2 glasses is demonstrated in Figure 6b. It is obvious that most data are consistent with the reference values within 5–10% for major elements and 10–20% for trace elements, proving the reliability of our method for analysis of granitoids. Exceptions include Cr, Co and Ni, which showed large bias from the reference values. Due to the relatively low concentrations (reference values: Cr: 20 µg g^{-1}; Co: 7.3 µg g^{-1}; Ni: 17 µg g^{-1}), these elements are easily affected by loss to Mo or

Table 3.
Results for GSP-2 glasses fused at 1550 °C and 1600 °C (25, 30 and 35 min)

Sample name			GSP-2													
Element	Isotope	Unit	Ref. value		1550 °C, 25 min		1550 °C, 30 min		1550 °C, 35 min		1600 °C, 25 min		1600 °C, 30 min		1600 °C, 35 min	
			Conc.	1 *s*	Ave., *n* = 15	1 *s*	Ave., *n* = 15	1 *s*	Ave., *n* = 15	1 *s*	Ave., *n* = 15	1 *s*	Ave., *n* = 15	1 *s*	Ave., *n* = 15	1 *s*
SiO_2	29	% *m/m*	66.6	0.8	66.9	0.5	67.0	0.6	67.1	0.7	66.8	0.3	67.4	0.5	67.1	0.4
TiO_2	48	% *m/m*	0.66	0.02	0.63	0.02	0.65	0.05	0.65	0.04	0.66	0.02	0.68	0.05	0.67	0.02
Al_2O_3	27	% *m/m*	14.9	0.2	15.5	0.2	15.6	0.4	15.5	0.4	15.9	0.2	15.9	0.4	15.9	0.1
FeO (total)	57	% *m/m*	4.41	0.14	4.57	0.29	4.14	0.20	4.29	0.18	4.08	0.22	3.93	0.38	4.19	0.16
MnO	55	% *m/m*	0.041	0.0026	0.04	0.001	0.04	0.002	0.04	0.002	0.04	0.001	0.04	0.002	0.04	0.001
MgO	25	% *m/m*	0.96	0.03	0.93	0.02	0.91	0.04	0.91	0.04	0.98	0.02	0.95	0.05	0.98	0.02
CaO	43	% *m/m*	2.1	0.06	2.18	0.08	2.23	0.13	2.23	0.11	2.27	0.08	2.19	0.12	2.22	0.08
Na_2O	23	% *m/m*	2.78	0.09	2.87	0.03	2.86	0.04	2.87	0.04	2.88	0.01	2.85	0.04	2.85	0.03
K_2O	39	% *m/m*	5.38	0.14	5.47	0.08	5.67	0.05	5.58	0.04	5.41	0.14	5.29	0.07	5.26	0.11
P_2O_5	31	% *m/m*	0.29	0.02	0.31	0.03	0.32	0.04	0.29	0.03	0.31	0.02	0.30	0.03	0.29	0.03
Li	7	$\mu g\ g^{-1}$	36	1	36.4	0.9	36.0	1.4	38.8	1.6	36.8	1.2	36.1	1.4	37.0	1.1
Sc	45	$\mu g\ g^{-1}$	6.3	0.7	7.20	0.95	6.87	0.44	6.88	0.40	7.28	0.47	7.04	0.40	7.09	0.45
V	51	$\mu g\ g^{-1}$	52	4	52.9	1.4	53.4	1.9	53.4	1.8	56.2	0.9	55.5	3.2	56.4	1.7
Cr	53	$\mu g\ g^{-1}$	20	6	24.1	6.6	38.1	13.8	21.3	6.3	30.3	3.9	30.9	2.2	62.9	20.6
Co	59	$\mu g\ g^{-1}$	7.3	0.8	5.44	0.78	4.14	1.12	4.31	0.98	5.01	0.87	4.18	1.13	3.72	1.07
Ni	60	$\mu g\ g^{-1}$	17	2	3.00	0.87	2.66	1.06	1.99	0.76	3.85	1.36	3.64	1.50	4.47	1.29
Cu	63	$\mu g\ g^{-1}$	43	4	39.4	3.1	44.4	2.1	39.8	2.7	40.2	1.2	38.4	1.9	41.4	1.6
Zn	66	$\mu g\ g^{-1}$	120	10	106	4	90	14	101	10	95	15	89	24	89	16
Ga	71	$\mu g\ g^{-1}$	22	2	25.0	1.0	22.4	3.0	23.3	1.4	23.7	2.2	19.9	5.4	21.5	2.6
Rb	85	$\mu g\ g^{-1}$	245	7	239	2	243	3	239	2	246	3	244	3	242	2
Sr	88	$\mu g\ g^{-1}$	240	10	247	7	247	10	246	13	253	3	249	10	255	4
Y	89	$\mu g\ g^{-1}$	28	2	26.5	1.4	27.3	1.6	27.1	1.6	27.2	0.4	27.3	1.2	27.2	0.6
Zr	91	$\mu g\ g^{-1}$	550	30	627	468	545	107	515	98	624	187	536	83	630	241
Nb	93	$\mu g\ g^{-1}$	27	2	27.2	0.9	27.9	1.9	27.6	1.4	28.7	0.8	28.7	1.6	28.8	0.9
Cs	133	$\mu g\ g^{-1}$	1.2	0.1	1.35	0.12	1.38	0.12	1.32	0.16	1.22	0.09	1.22	0.10	1.21	0.10
Ba	137	$\mu g\ g^{-1}$	1340	44	1356	36	1368	55	1349	56	1410	14	1385	49	1405	19
La	139	$\mu g\ g^{-1}$	180	12	180	12	189	14	189	13	194	4	191	8	191	4
Ce	140	$\mu g\ g^{-1}$	410	30	437	29	457	35	460	31	466	10	462	18	461	9
Pr	141	$\mu g\ g^{-1}$	54[a]	3	53.4	3.6	56.1	4.2	56.3	3.9	58.1	1.2	57.6	2.3	57.6	1.2
Nd	143	$\mu g\ g^{-1}$	200	12	207	15	216	17	217	16	216	5	214	8	215	4
Sm	147	$\mu g\ g^{-1}$	27	1	25.9	1.8	26.9	2.1	27.2	2.1	27.9	0.7	27.4	1.4	27.2	0.9
Eu	151	$\mu g\ g^{-1}$	2.3	0.1	2.32	0.12	2.35	0.11	2.34	0.17	2.37	0.10	2.33	0.10	2.40	0.12
Gd[b]	155	$\mu g\ g^{-1}$	12	2	14.6	1.0	15.2	1.0	15.2	1.2	15.3	0.5	15.2	0.8	15.3	0.4
Gd[c]	155	$\mu g\ g^{-1}$	12	2	12.0	1.0	12.5	1.1	12.5	1.2	12.6	0.5	12.6	0.8	12.6	0.4
Tb	159	$\mu g\ g^{-1}$	1.36[a]	0.07	1.29	0.06	1.35	0.09	1.36	0.10	1.54	0.04	1.53	0.08	1.51	0.03

GEOSTANDARDS and GEOANALYTICAL RESEARCH

GEOSTANDARDS and GEOANALYTICAL RESEARCH

Table 3 (continued).
Results for GSP-2 glasses fused at 1550 °C and 1600 °C (25, 30 and 35 min)

Sample name			GSP-2													
Element	Isotope	Unit	Ref. value		1550 °C, 25 min		1550 °C, 30 min		1550 °C, 35 min		1600 °C, 25 min		1600 °C, 30 min		1600 °C, 35 min	
			Conc.	1*s*	Ave., *n* = 15	1*s*	Ave., *n* = 15	1*s*	Ave., *n* = 15	1*s*	Ave., *n* = 15	1*s*	Ave., *n* = 15	1*s*	Ave., *n* = 15	1*s*
Dy	163	μg g^{-1}	6.1	–	5.67	0.43	5.81	0.44	5.84	0.41	6.41	0.28	6.42	0.31	6.31	0.25
Ho	165	μg g^{-1}	1	0.1	0.97	0.07	0.98	0.07	1.00	0.05	1.00	0.08	1.02	0.04	1.00	0.03
Er	166	μg g^{-1}	2.37[a]	0.09	2.48	0.19	2.55	0.15	2.53	0.20	2.76	0.11	2.73	0.22	2.77	0.13
Tm	169	μg g^{-1}	0.29	0.02	0.27	0.02	0.29	0.02	0.29	0.03	0.31	0.01	0.31	0.03	0.29	0.02
Yb	173	μg g^{-1}	1.6	0.2	1.75	0.18	1.75	0.17	1.71	0.18	1.81	0.09	1.72	0.10	1.85	0.11
Lu	175	μg g^{-1}	0.23	0.03	0.23	0.03	0.23	0.02	0.23	0.03	0.26	0.02	0.24	0.03	0.25	0.02
Hf	178	μg g^{-1}	14	1	16.3	13.2	14.0	2.8	13.4	2.5	15.5	4.3	13.2	2.3	15.6	6.0
Ta	181	μg g^{-1}	0.9[a]	0.1	0.86	0.07	0.92	0.09	0.92	0.09	0.98	0.07	1.00	0.11	0.99	0.07
Pb	208	μg g^{-1}	42	3	46.8	3.4	39.2	6.1	42.0	4.2	39.7	6.5	38.4	10.6	37.3	7.3
Th	232	μg g^{-1}	105	8	104	9	114	9	113	11	113	3	111	4	111	3
U	238	μg g^{-1}	2.4	0.19	2.39	0.28	2.59	0.20	2.52	0.24	2.62	0.12	2.52	0.12	2.61	0.13

[a]The reference values of Pr, Tb, Er and Ta were taken from Cotta and Enzweiler (2012); [b]Uncorrected Gd data; [c]Corrected Gd data.

contamination during prolonged heating. We also note that loss of volatile elements (e.g., Pb, Zn and Cs) was minor (< 10–20%), and elements such as Zr, Hf and the HREEs (which are compatible in zircon) are in agreement with the reference values within error of 10–20%.

One issue during determination of REE by LA-ICP-MS is the isobaric interferences of Ba and LREE oxides on middle rare earth elements (MREEs; e.g., Eu and Gd), and these interferences can be exacerbated by high contents of Ba (relative to Eu) and La, Ce and Pr (relative to Gd) (Kent and Ungerer 2005). GSP-2 has a high La/Gd ratio (~ 15), so the isobaric interferences from La oxides should be evaluated. The measured Gd contents in GSP-2 are systematically higher than the reference values by 25% (Table 3), and probably caused by the isobaric interference of $^{139}La^{16}O$ on ^{155}Gd. The calculation by Kent and Ungerer (2005) showed that the $^{139}La^{16}O/^{139}La$ is about 80% of the maximum oxide production rate as presented by ThO^+/Th^+. We estimate that the $^{139}La^{16}O/^{139}La$ was around 1.2–1.6% in our study, given that the optimised ThO^+/Th^+ was about 1.5–2%. Therefore, the Gd data can be corrected by subtracting the contribution of $^{139}La^{16}O$ to ^{155}Gd assuming that the $^{139}La^{16}O/^{139}La$ is ~ 1.4%. The corrected Gd contents are consistent with the USGS reference data (Table 3). We also suggest that ^{157}Gd should be used for measurement of Gd concentration because PrO^+/Pr^+ production is relatively low and Pr abundances are lower than La and Ce (Kent and Ungerer 2005). As contributions from BaO to Eu are significant only for samples with Ba/Eu ratios higher than 1000 (Kent and Ungerer 2005), Eu content was not corrected for BaO interference for analysis of GSP-2 glass due to its low Ba/Eu ratio (~ 580).

Overall, our method provided reliable LA-ICP-MS data for granitoids. One of the advantages of the method is that it avoids tedious wet chemistry digestion procedures, high-purity MgO or fluxes (e.g., $LiBO_2$ and $Li_2B_4O_7$) to melt high-SiO_2 samples for conventional solution ICP-MS and LA-ICP-MS methods (Nehring *et al.* 2008, Park *et al.* 2013). In routine analysis, melting at 1550 °C and 30 min is recommended to obtain homogeneous glasses although small amounts of residual zircon (10–20 μm) were preserved in high-SiO_2 powders.

Analytical results for basalts, andesite, rhyolite and diabase

To investigate the data quality from LA-ICP-MS in combination with our flux-free fusion technique, several USGS extrusive rock RMs including BHVO-2, BIR-1, AGV-1 and RGM-1 were measured. The recommended melting condition (1450 °C, 10 min) was applied to all samples. The diabase reference material W-2 was also fused under the same condition to test its suitability for mafic intrusive rocks. Figure 2c, d shows the morphology of RGM-1 and W-2 glasses fused at 1450 °C for 10 min. To examine elemental homogeneity, W-2 was investigated along a profile (A–B) by LA-ICP-MS (Figure 2d). Figure 7 shows that elements were homogenously distributed along the profile and the composition was consistent with reference data, implying that this melting condition is feasible for diabase. As the liquidus of mafic intrusive rocks such as gabbro and amphibolite is lower than 1450 °C at ambient pressure, our method could also be useful for other mafic intrusive rocks, but could not be applied to high-Mg mafic–ultramafic rocks (such as peridotites) because of their high liquidus values.

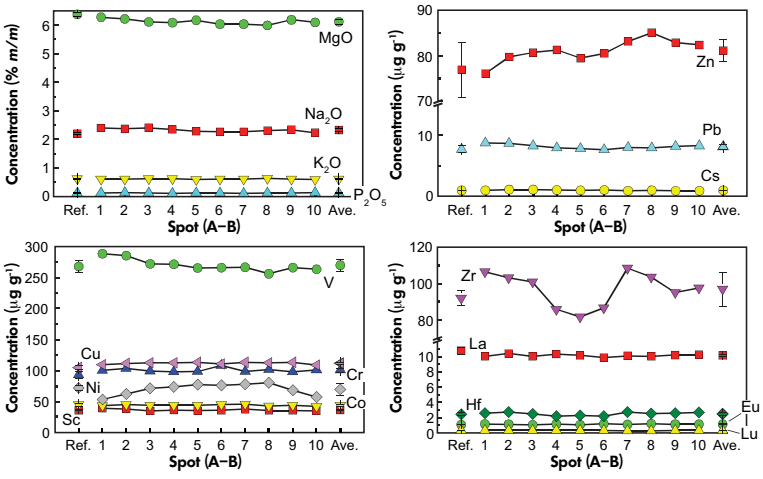

Figure 7. Element distributions along the A–B profile of the W-2 glass fused at 1450 °C for 10 min. The A–B profile is shown in Figure 2 (d). Ref., reference values with 1*s* uncertainty; Ave., average values with 1*s* uncertainty.

Table 4.
Results for BHVO-2, BIR-1, AGV-1, W-2 and RGM-1 glasses fused under optimum conditions (1450 °C and 10 min)

Sample name			BHVO-2				BIR-1				AGV-1			
Element	Isotope	Unit	Ref. value		1450 °C, 10 min		Ref. value		1450 °C, 10 min		Ref. value		1450 °C, 10 min	
			Conc.	1 *s*	Ave., *n* = 10	1 *s*	Conc.	1 *s*	Ave., *n* = 10	1 *s*	Conc.	1 *s*	Ave., *n* = 10	1 *s*
SiO_2	29	% *m/m*	49.9	0.6	49.8	0.4	47.7	0.4	48.3	0.4	58.84	0.58	59.6	0.7
TiO_2	48	% *m/m*	2.73	0.04	2.75	0.04	0.97	0.03	0.88	0.01	1.05	0.05	1.04	0.10
Al_2O_3	27	% *m/m*	13.5	0.2	13.6	0.2	15.4	0.2	15.5	0.1	17.15	0.34	17.9	0.3
FeO (total)	57	% *m/m*	11.4	-	11.9	0.2	10.6	0.4	10.77	0.17	6.09	0.17	6.53	0.29
MnO	55	% *m/m*	0.17	0.005	0.18	0.00	0.176	0.008	0.18	0.002	0.097	0.005	0.10	0.00
MgO	25	% *m/m*	7.23	0.12	6.80	0.19	9.7	0.1	9.08	0.10	1.53	0.093	1.55	0.05
CaO	43	% *m/m*	11.4	0.2	11.3	0.4	13.4	0.2	12.7	0.3	4.94	0.14	5.04	0.19
Na_2O	23	% *m/m*	2.22	0.08	2.24	0.03	1.81	0.03	1.87	0.03	4.26	0.12	4.39	0.11
K_2O	39	% *m/m*	0.52	0.01	0.50	0.01	0.03	0.003	0.02	0.001	2.92	0.37	2.95	0.08
P_2O_5	31	% *m/m*	0.27	0.02	0.28	0.01	0.027	0.007	0.02	0.01	0.5	0.03	0.51	0.02
Li	7	$\mu g\ g^{-1}$	4.8	0.2	4.11	0.47	3.2	0.2	2.90	0.31	10.7	0.9	9.86	0.56
Sc	45	$\mu g\ g^{-1}$	32	1	32.0	1.2	43	2	40.9	0.8	12.3	0.5	12.0	0.7
V	51	$\mu g\ g^{-1}$	317	11	315	4	319	18	308	4	119	6	123	15
Cr	53	$\mu g\ g^{-1}$	280	19	288	8	391	15	397	15	9.4	1.2	16.8	8.2
Co	59	$\mu g\ g^{-1}$	45	3	44.0	1.0	52	3	50.8	0.6	15.2	0.9	15.2	0.7
Ni	60	$\mu g\ g^{-1}$	119	7	108	7	166	7	155	14	15.5	0.8	23.0	7.8
Cu	63	$\mu g\ g^{-1}$	127	7	134	3	119	8	127	2	58	2	60.9	1.5
Zn	66	$\mu g\ g^{-1}$	103	6	107	4	72	18	68.0	3.5	87	4	90.8	5.1
Ga	71	$\mu g\ g^{-1}$	22	2	22.1	0.9	15.3	0.8	15.6	0.7	20.2	0.5	21.3	0.8
Rb	85	$\mu g\ g^{-1}$	9.11	0.04	8.87	0.32	0.2	0.01	0.21	0.03	66.6	0.4	68.6	1.5
Sr	88	$\mu g\ g^{-1}$	396	1	392	4	109	2	106	1	660	6	699	17
Y	89	$\mu g\ g^{-1}$	26	2	24.9	0.3	15.6	0.9	14.3	0.3	19	1	18.6	0.8
Zr	91	$\mu g\ g^{-1}$	172	11	170	5	14	0.1	13.8	0.5	231	9	232	12
Nb	93	$\mu g\ g^{-1}$	18.1	1	18.2	0.5	0.55	0.05	0.52	0.05	14.6	1	15.0	0.9
Cs	133	$\mu g\ g^{-1}$	0.1	0.01	0.13	0.05	0.007	0.003	0.03	0.03	1.26	0.07	1.40	0.08
Ba	137	$\mu g\ g^{-1}$	131	1	132	3	7.14	-	6.42	0.65	1200	8	1280	39
La	139	$\mu g\ g^{-1}$	15.2	0.1	15.0	0.3	0.615	0.021	0.66	0.08	38.2	0.04	38.9	1.3
Ce	140	$\mu g\ g^{-1}$	37.5	0.2	37.7	0.7	1.92	0.08	1.88	0.08	67.6	1.1	72.3	2.6
Pr	141	$\mu g\ g^{-1}$	5.35	0.17	5.26	0.13	0.37	0.02	0.36	0.05	8.3	0.5	8.44	0.34
Nd	143	$\mu g\ g^{-1}$	24.5	0.1	24.6	1.3	2.38	0.01	2.26	0.19	31.7	0.1	32.7	1.8
Sm	147	$\mu g\ g^{-1}$	6.07	0.01	6.11	0.23	1.12	0.02	1.08	0.16	5.72	0.03	5.93	0.47
Eu	151	$\mu g\ g^{-1}$	2.07	0.02	2.11	0.06	0.53	-	0.50	0.04	1.58	0.02	1.79	0.06
Gd	155	$\mu g\ g^{-1}$	6.24	0.03	6.26	0.22	1.87	0.04	1.71	0.18	4.7	0.05	5.23	0.29
Tb	159	$\mu g\ g^{-1}$	0.92	0.03	0.94	0.04	0.36	0.03	0.34	0.02	0.69	0.04	0.67	0.02
Dy	163	$\mu g\ g^{-1}$	5.31	0.02	5.36	0.16	2.51	-	2.51	0.12	3.55	0.03	3.75	0.20

Table 4 (continued).
Results for BHVO-2, BIR-1, AGV-1, W-2 and RGM-1 glasses fused under optimum conditions (1450 °C and 10 min)

Sample name			BHVO-2				BIR-1				AGV-1			
Element	Isotope	Unit	Ref. value		1450 °C, 10 min		Ref. value		1450 °C, 10 min		Ref. value		1450 °C, 10 min	
			Conc.	1 *s*	Ave., *n* = 10	1 *s*	Conc.	1 *s*	Ave., *n* = 10	1 *s*	Conc.	1 *s*	Ave., *n* = 10	1 *s*
Ho	165	µg g^{-1}	0.98	0.04	1.00	0.05	0.56	0.05	0.54	0.03	0.68	0.03	0.70	0.05
Er	166	µg g^{-1}	2.54	0.01	2.49	0.12	1.66	-	1.62	0.06	1.82	0.02	1.85	0.14
Tm	169	µg g^{-1}	0.33	0.01	0.32	0.03	0.25	0.03	0.23	0.02	0.28	0.02	0.25	0.02
Yb	173	µg g^{-1}	2	0.01	1.96	0.12	1.65	-	1.64	0.13	1.63	0.02	1.69	0.12
Lu	175	µg g^{-1}	0.274	0.005	0.29	0.02	0.25	0.02	0.25	0.01	0.244	0.002	0.26	0.02
Hf	178	µg g^{-1}	4.36	0.14	4.31	0.10	0.582	0.004	0.54	0.05	5.1	0.2	5.08	0.36
Ta	181	µg g^{-1}	1.14	0.06	1.13	0.05	0.0357	0.0004	0.04	0.01	0.87	0.05	0.88	0.06
Pb	208	µg g^{-1}	1.6	0.3	1.64	0.07	3.1	0.3	3.22	0.17	37.4	2.9	41.0	2.7
Th	232	µg g^{-1}	1.22	0.06	1.21	0.04	0.032	0.004	0.03	0.01	6.4	0.3	6.46	0.25
U	238	µg g^{-1}	0.403	0.001	0.40	0.03	0.01	0.001	0.01	0.003	1.93	0.06	1.90	0.094

Sample name			W-2				RGM-1			
Element	Isotope	Unit	Ref. value		1450 °C, 10 min		Ref. value		1450 °C, 10 min	
			Conc.	1 *s*	Ave., *n* = 10	1 *s*	Conc.	1 *s*	Ave., *n* = 10	1 *s*
SiO_2	29	% *m/m*	52.68	0.29	52.6	0.5	73.4	0.53	73.3	0.2
TiO_2	48	% *m/m*	1.06	0.01	1.10	0.07	0.27	0.02	0.27	0.01
Al_2O_3	27	% *m/m*	15.45	0.16	15.5	0.3	13.7	0.19	14.6	0.2
FeO (total)	57	% *m/m*	9.74	0.19	10.4	0.2	1.67	0.03	1.76	0.11
MnO	55	% *m/m*	0.167	0.004	0.18	0.00	0.036	0	0.04	0.00
MgO	25	% *m/m*	6.37	0.058	6.12	0.09	0.28	0.03	0.26	0.01
CaO	43	% *m/m*	10.86	0.078	10.8	0.1	1.15	0.07	1.32	0.07
Na_2O	23	% *m/m*	2.2	0.037	2.32	0.06	4.07	0.15	3.95	0.06
K_2O	39	% *m/m*	0.626	0.012	0.62	0.01	4.3	0.1	4.25	0.06
P_2O_5	31	% *m/m*	0.13	0.03	0.13	0.01	0.048	0.02	0.05	0.01
Li	7	µg g^{-1}	9.3	0.4	8.63	0.95	57	8	56.3	1.4
Sc	45	µg g^{-1}	35.9	0.8	36.3	1.4	4.4	0.3	5.12	0.33
V	51	µg g^{-1}	268	10	270	10	13	2	11.5	0.5
Cr	53	µg g^{-1}	93	6	101	3	5.74	–	2.75	0.91
Co	59	µg g^{-1}	45	2	44.0	1.1	2	0.2	1.82	0.13
Ni	60	µg g^{-1}	72	4	69.7	9.3	4.4	–	2.87	0.46
Cu	63	µg g^{-1}	105	3	112	2	11.6	1.4	11.5	0.9
Zn	66	µg g^{-1}	77	6	81.2	2.5	32	–	32.7	1.4
Ga	71	µg g^{-1}	18	1	19.0	0.7	15	2	16.0	1.6
Rb	85	µg g^{-1}	21	1	20.0	0.7	150	8	141.5	2.8

GEOSTANDARDS and GEOANALYTICAL RESEARCH

Table 4 (continued).
Results for BHVO-2, BIR-1, AGV-1, W-2 and RGM-1 glasses fused under optimum conditions (1450 °C and 10 min)

Sample name			W-2				RGM-1			
Element	Isotope	Unit	Ref. value		1450 °C, 10 min		Ref. value		1450 °C, 10 min	
			Conc.	1*s*	Ave., *n* = 10	1*s*	Conc.	1*s*	Ave., *n* = 10	1*s*
Sr	88	μg g^{-1}	196	5	194	3	110	10	111.9	2.4
Y	89	μg g^{-1}	22	1	20.3	0.5	25	–	24.0	0.5
Zr	91	μg g^{-1}	92	4	97.0	9.3	220	20	245	5
Nb	93	μg g^{-1}	7.5	0.6	7.38	0.28	8.9	0.6	9.70	0.34
Cs	133	μg g^{-1}	0.92	0.07	0.96	0.07	9.6	0.6	10.3	0.3
Ba	137	μg g^{-1}	172	7	170	3	810	46	877	18
La	139	μg g^{-1}	10.8	0.5	10.2	0.2	24	1.1	24	1
Ce	140	μg g^{-1}	23.4	0.7	23.2	0.4	47	4	48	1
Pr	141	μg g^{-1}	3	0.1	2.84	0.11	5.36	–	5.44	0.13
Nd	143	μg g^{-1}	13	0.5	13.2	0.5	19	1	20.4	0.8
Sm	147	μg g^{-1}	3.3	0.08	3.20	0.29	4.3	0.3	4.17	0.33
Eu	151	μg g^{-1}	1.08	0.03	1.14	0.05	0.66	0.08	0.64	0.05
Gd	155	μg g^{-1}	3.66	0.12	3.65	0.17	3.7	0.4	4.21	0.27
Tb	159	μg g^{-1}	0.62	0.03	0.62	0.04	0.66	–	0.62	0.03
Dy	163	μg g^{-1}	3.79	0.09	3.92	0.13	4.1	0.1	4.03	0.15
Ho	165	μg g^{-1}	0.79	0.03	0.80	0.04	0.82	–	0.82	0.04
Er	166	μg g^{-1}	2.22	0.1	2.13	0.10	2.35	–	2.48	0.14
Tm	169	μg g^{-1}	0.33	0.02	0.30	0.01	0.37	–	0.38	0.03
Yb	173	μg g^{-1}	2.05	0.04	2.09	0.14	2.6	0.3	2.81	0.19
Lu	175	μg g^{-1}	0.31	0.01	0.31	0.02	0.4	0.03	0.43	0.02
Hf	178	μg g^{-1}	2.45	0.18	2.50	0.20	6.2	–	6.34	0.15
Ta	181	μg g^{-1}	0.47	0.04	0.44	0.03	0.95	0.1	1.02	0.06
Pb	208	μg g^{-1}	7.7	0.6	8.13	0.36	23.6	3	24.6	0.9
Th	232	μg g^{-1}	2.17	0.09	2.17	0.11	15.1	1.3	15.6	0.4
U	238	μg g^{-1}	0.51	0.02	0.48	0.05	5.8	0.5	5.63	0.19

The reference values for BHVO-2, BIR-1, AGV-1 and W-2 were taken from the preferred values in the GeoReM database (http://georem.mpch-mainz.gwdg.de/); the reference values for RGM-1 were taken from GeoReM database, which were cited by Zhu *et al.* (2013).

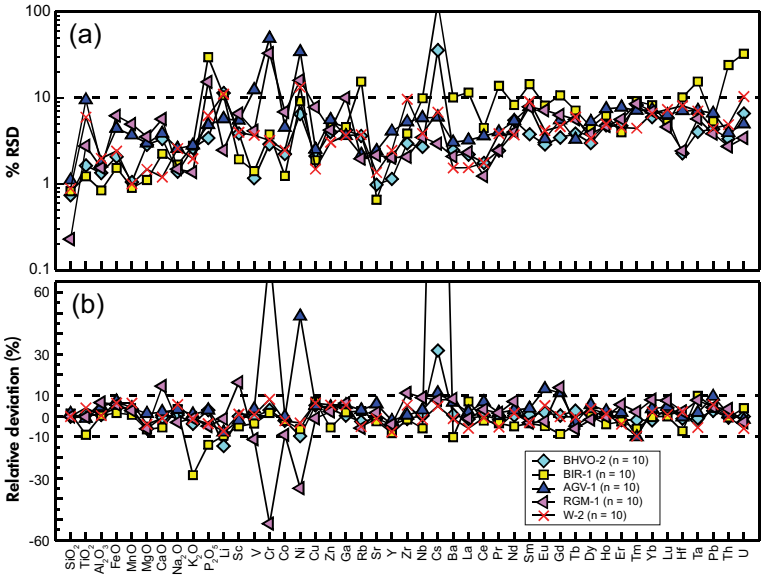

Figure 8. (a) RSD and (b) relative deviations of the measured values from the reference values for BHVO-2, BIR-1, AGV-1, RGM-1 and W-2 glasses fused at the optimum melting condition (1450 °C and 10 min).

As shown in Table 4 and Figure 8, the data quality of our results is comparable to conventional methods. LA-ICP-MS data for BHVO-2, BIR-1, AGV-1, RGM-1 and W-2 generally agree with the recommended values within a discrepancy of 5% for major elements and 5–10% for trace elements, with precision better than 5–10% RSD for most elements. Interferences of $^{28}Si^{17}O$ and $^{29}Si^{16}O$ on ^{45}Sc, $^{135}Ba^{16}O$ on ^{151}Eu and $^{139}La^{16}O$ on ^{155}Gd do not cause clear bias due to relatively low oxide interferences for BHVO-2, BIR-1, AGV-1, RGM-1 and W-2 (Figure 8b). Corrections were thus not applied for the LA-ICP-MS data.

The LA-ICP-MS data in Figure 8 indicate that our method has limitations in determining elements with low concentrations. Taking BIR-1 as an example, these elements mainly include K_2O (0.03% *m/m*), P_2O_5 (0.027% *m/m*), Cs (0.007 μg g^{-1}), Ta (0.0357 μg g^{-1}), Th (0.032 μg g^{-1}) and U (0.01 μg g^{-1}) (from the GeoReM database). As shown in Figure 9, negative correlations between concentrations and RSDs were found in BIR-1, BHVO-2, AGV-1 and RGM-1 for most elements. The trend of decreasing RSD with increasing concentration reveals the relationship between analytical precision and counting statistics. To obtain accurate concentration data, chemical heterogeneities for elements in the glass should be smaller than analytical uncertainty (Gao *et al.* 2002, Luo *et al.* 2007, Hu *et al.* 2009). This also shows that Cr and Ni in AGV-1 and RGM-1 lie beyond the negative correlation trends (Figure 9), which may be due to heterogeneous distributions in the glasses. Similar to GSP-2, the high RSD and large bias in LA-ICP-MS

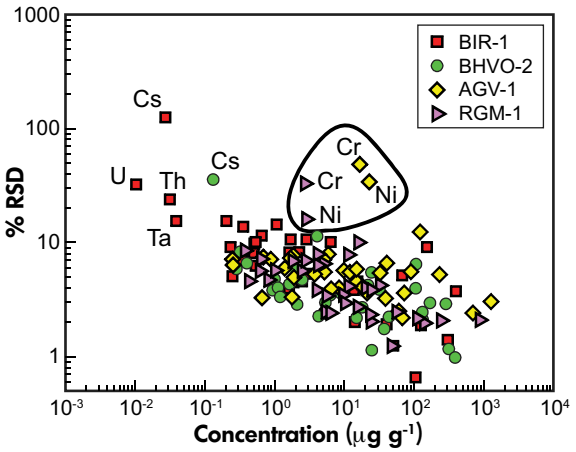

Figure 9. Correlations between RSD values and trace element concentrations for BIR-1, BHVO-2, AGV-1 and RGM-1 glasses fused at 1450 °C for 10 min.

data for Cr and Ni in AGV-1 and RGM-1 may be also susceptible to the fusion process due to their low concentrations (Figure 8). In contrast, results for Cr and Ni in BHVO-2, BIR-1 and W-2 with relatively high contents (100–400 μg g^{-1} for Cr and 69–400 μg g^{-1} for Ni) generally showed low RSD values and no significant bias (Figure 8). This indicates that heterogeneity of Cr and Ni caused by the fusion process is smaller than the analytical uncertainties of LA-ICP-MS when their concentrations are high enough. The high RSD values of Cs, Ta, Th and U in BIR-1 and Cs (0.1 μg g^{-1}) in BHVO-2 reflect low signal intensities during ICP-MS analy-

Table 5.
Comparison of major and trace element concentrations of two natural samples (basalt 13AFS-2 and granodiorite 06TG-1) obtained by our method and those obtained from XRF and solution ICP-MS for 13AFS-2, XRF and LA-ICP-MS after flux-fusion for 06TG-1

Sample name			13AFS-2 (Basalt)				06TG-1 (Granodiorite)			
Element	Isotope	Unit	XRF and SN-ICP-MS	1450 °C, 10 min			XRF and LA-ICP-MS	1550 °C, 30 min		
			Conc.	Ave. (n = 6)	% RSD	RD (%)	Conc.	Ave. (n = 11)	% RSD	RD (%)
SiO_2	29	% m/m	44.4	43.9	0.6	-1.2	61.1	61.7	1.7	1.0
TiO_2	48	% m/m	2.37	2.35	0.6	-0.7	0.68	0.64	3.7	-5.7
Al_2O_3	27	% m/m	12.0	12.2	0.6	1.7	18.4	18.9	2.9	2.5
FeO (total)	57	% m/m	11.2	11.5	1.6	2.3	3.61	3.57	4.3	-1.0
MnO	55	% m/m	0.20	0.20	0.7	-0.7	0.06	0.07	5.2	5.7
MgO	25	% m/m	7.24	7.29	0.9	0.8	1.51	1.41	5.3	-6.7
CaO	43	% m/m	8.74	8.99	1.3	2.8	4.49	4.82	5.7	7.5
Na_2O	23	% m/m	6.22	6.49	0.3	4.4	4.95	5.11	0.8	3.2
K_2O	39	% m/m	2.78	2.86	0.4	2.8	2.91	2.91	2.1	-0.1
P_2O_5	31	% m/m	1.42	1.50	0.9	5.7	0.26	0.32	4.9	24.1
Li	7	µg g^{-1}	17.8	13.4	2.3	-24.8	–	11.3	4.4	-
Sc	45	µg g^{-1}	12.8	11.0	3.6	-13.9	10.0	9.06	4.7	-9.4
V	51	µg g^{-1}	120	118	0.5	-1.8	62.0	59.1	4.7	-4.7
Cr	53	µg g^{-1}	114	115	2.3	1.0	9.00	23.5	24.7	161.1
Co	59	µg g^{-1}	40.0	37.4	0.7	-6.5	11.0	8.62	15.4	-21.6
Ni	60	µg g^{-1}	108	92.5	4.6	-14.2	7.00	2.45	95.1	-65.1
Cu	63	µg g^{-1}	36.2	37.4	2.9	3.4	5.00	9.09	7.4	81.8
Zn	66	µg g-	–	176	0.9	–	65.0	60.7	15.3	-6.6
Ga	71	µg g^{-1}	29.4	27.6	1.4	-6.1	22.0	23.6	8.2	7.1
Rb	85	µg g^{-1}	39.3	37.5	1.1	-4.6	59.6	54.9	3.0	-7.8
Sr	88	µg g^{-1}	1632	1690	1.0	3.5	1026	1042	5.1	1.6
Y	89	µg g^{-1}	43.7	42.6	1.2	-2.4	17.2	16.8	6.9	-2.5
Zr	91	µg g^{-1}	423	415	1.4	-1.7	196	301	96.7	-2.4
Nb	93	µg g^{-1}	139	142	0.7	2.7	10.6	10.2	7.9	-3.5
Cs	133	µg g^{-1}	1.86	1.74	5.9	-6.8	1.43	1.47	7.9	3.2
Ba	137	µg g^{-1}	701	696	1.1	-0.8	2247	2245	4.5	-0.1
La	139	µg g^{-1}	92.1	91.9	1.0	-0.2	45.7	43.4	8.7	-5.0
Ce	140	µg g^{-1}	169	171	0.6	1.3	89.4	89.4	7.5	0.0
Pr	141	µg g^{-1}	18.5	19.4	1.2	4.7	10.4	10.4	7.8	0.4
Nd	143	µg g^{-1}	82.1	79.9	1.3	-2.8	39.7	37.9	7.2	-4.7
Sm	147	µg g^{-1}	17.7	16.3	4.1	-8.3	6.57	6.89	10.6	4.8
Eu	151	µg g^{-1}	5.09	5.06	1.8	-0.6	2.28	2.29	9.9	0.5
Gd	155	µg g^{-1}	19.4	15.2	2.9	-21.5	4.96	5.03	7.2	1.5
Tb	159	µg g^{-1}	2.10	1.99	3.2	-5.5	0.65	0.66	9.5	0.5

Table 5 (continued).
Comparison of major and trace element concentrations of two natural samples (basalt 13AFS-2 and granodiorite 06TG-1) obtained by our method and those obtained from XRF and solution ICP-MS for 13AFS-2, XRF and LA-ICP-MS after flux-fusion for 06TG-1

Sample name			13AFS-2 (Basalt)				06TG-1 (Granodiorite)			
Element	Isotope	Unit	XRF and SN-ICP-MS	1450 °C, 10 min			XRF and LA-ICP-MS	1550 °C, 30 min		
			Conc.	Ave. (n = 6)	% RSD	RD (%)	Conc.	Ave. (n = 11)	% RSD	RD (%)
Dy	163	μg g^{-1}	9.57	9.85	2.5	2.9	3.27	3.24	7.2	-0.9
Ho	165	μg g^{-1}	1.49	1.60	1.1	7.0	0.59	0.59	8.2	0.2
Er	166	μg g^{-1}	3.35	3.52	5.4	5.1	1.51	1.65	10.0	9.6
Tm	169	μg g^{-1}	0.39	0.42	6.4	6.6	0.23	0.22	14.6	-2.9
Yb	173	μg g^{-1}	2.45	2.32	4.6	-5.2	1.36	1.45	10.3	6.4
Lu	175	μg g^{-1}	0.35	0.32	6.5	-8.8	0.20	0.22	20.2	8.7
Hf	178	μg g^{-1}	8.11	8.62	2.7	6.3	4.50	6.70	95.7	-2.5
Ta	181	μg g^{-1}	7.08	7.06	1.5	-0.4	0.79	0.75	9.8	-5.0
Pb	208	μg g^{-1}	7.55	6.51	2.3	-13.7	16.5	17.2	15.8	3.7
Th	232	μg g^{-1}	13.8	13.9	0.7	0.3	4.9	4.5	12.3	-9.1
U	238	μg g^{-1}	3.27	3.00	1.7	-8.3	1.11	1.13	13.8	1.6

The concentration data for 13AFS-2 were obtained by XRF and SN-ICP-MS were taken from J. Huang, S.G. Li, Y.L. Xiao, S. Ke, W.Y. Li, Y. Tian (unpublished data); concentration data for 06TG-1 obtained by XRF and LA-ICP-MS were taken from He *et al.* (2011).

GEOSTANDARDS and GEOANALYTICAL RESEARCH

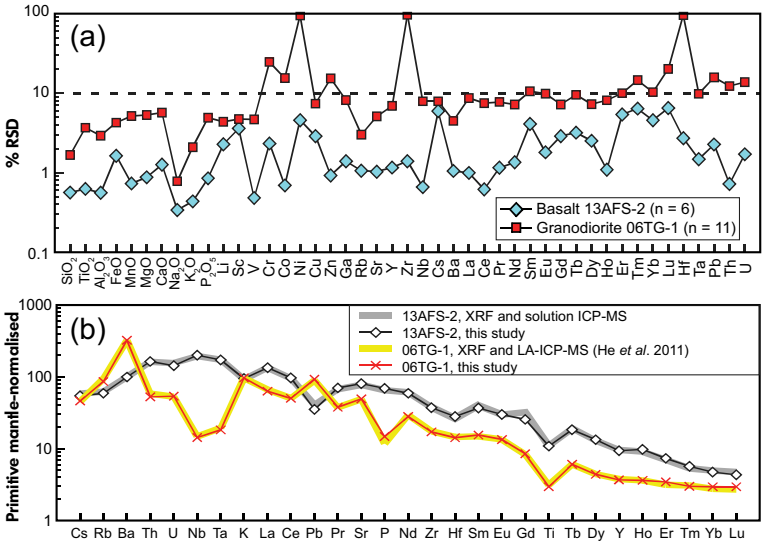

Figure 10. (a) Precision (RSD) of elemental contents of two natural samples (basalt 13AFS-2 and granodiorite 06TG-1) analysed by the method described in this study; (b) comparison of primitive mantle-normalised trace element concentrations of basalt 13AFS-2 and granodiorite 06TG-1 obtained from different methods.

ses, rather than chemical heterogeneity caused by the fusion process.

Comparison with other methods

To investigate further the potential of our flux-free fusion technique for routine bulk rock analysis, we fused two natural rock samples, basalt 13AFS-2 and granodiorite 06TG-1, under the recommended melting conditions of 1450 °C for 10 min and 1550 °C for 30 min, respectively. In Table 5, the results are compared with literature data obtained from other methods (XRF spectrometry, solution ICP-MS and LA-ICP-MS after flux-fusion) (He *et al.* 2011, J. Huang, S.G. Li, Y.L. Xiao, S. Ke, W.Y. Li, Y. Tian, unpublished data).

Figure 10a shows that the precision of our method was generally better than 5–10% RSD for 13AFS-2 and 06TG-1. Exceptions were Cr, Co, Ni, Zn, Zr, Hf and elements with low concentrations in granodiorite 06TG-1. The accuracy of the LA-ICP-MS data is demonstrated by the agreement of concentration data obtained by different techniques. As illustrated in Table 5, most LA-ICP-MS data for basalt 13AFS-2 and granodiorite 06TG-1 agree with values derived by XRF, solution ICP-MS and LA-ICP-MS after flux-fusion within a discrepancy of 10%. Figure 10b further shows that the primitive mantle-normalised trace element patterns derived from different methods match well (Sun and McDonough 1989). These observations suggest that the new flux-free fusion technique described herein can provide reliable elemental content data.

Conclusions

A new method was developed combining the flux-free fusion technique with LA-ICP-MS for rapid and accurate determinations of major and trace elements in silicate rocks. The advantage of our method is that homogeneous glasses can be obtained through melting rock powders at 1450–1600 °C in a normal one-atmosphere furnace without adding any flux agent. This simple technique minimises drawbacks causing analytical uncertainty, such as volatilisation, contamination and metal segregation (mainly Cr, Ni and Cu). Analytical results obtained for eight USGS reference materials and two natural samples using our method generally agree with recommended values within discrepancy of 5–10% for both major and trace elements. The analytical precision, as given by one RSD, was less than 5–10% for most elements. Therefore, this method has great potential to provide reliable and rapid analyses of major and trace element concentrations for silicate rocks, especially for extrusive rocks and most mafic to intermediate intrusive rocks.

Acknowledgements

We are grateful to Yongsheng He and Jian Huang for providing the natural powdered samples. Zhenhui Hou and Yerong Jiang are thanked for help in the laboratory. This work was supported by the National Science Foundation of China (41173031, 41325011 and 40873009, 41173009), the 111 Project, and the Fundamental Research Funds for the Central Universities.

References

Awaji S., Nakamura K., Nozaki T. and Kato Y. (2006)
A simple method for precise determination of 23 trace elements in granitic rocks by ICP-MS after lithium tetraborate fusion. Resource Geology, 56, 471–478.

Bayon G., Barrat J.A., Etoubleau J., Benoit M., Bollinger C. and Révillon S. (2009)
Determination of rare earth elements, Sc, Y, Zr, Ba, Hf and Th in geological samples by ICP-MS after Tm addition and alkaline fusion. Geostandards and Geoanalytical Research, 33, 51–62.

Brown R.W. (1977)
A sample fusion technique for whole rock analysis with the electron microprobe. Geochimica et Cosmochimica Acta, 41, 435–438.

Chen L., Liu Y.S., Hu Z.S., Gao S., Zong K.Q. and Chen H.H. (2011)
Accurate determinations of fifty-four major and trace elements in carbonate by LA-ICP-MS using normalization strategy of bulk components as 100%. Chemical Geology, 284, 283–295.

Cotta A.J.B. and Enzweiler J. (2012)
Classical and new procedures of whole rock dissolution for trace element determination by ICP-MS. Geostandards and Geoanalytical Research, 36, 27–50.

Eggins S.M. (2003)
Laser ablation ICP-MS analysis of geological materials prepared as lithium borate glasses. Geostandards Newsletter: The Journal of Geostandards and Geoanalysis, 27, 147–162.

Eggins S.M., Woodhead J.D., Kinsley L.P.J., Mortimer G.E., Sylvester P., McCulloch M.T., Hergt J.M. and Handler M.R. (1997)
A simple method for the precise determination of ≥ 40 trace elements in geological samples by ICP-MS using enriched isotope internal standardisation. Chemical Geology, 134, 311–326.

Fedorowich J.S., Richards J.P., Jain J.C., Kerrich R. and Fan J. (1993)
A rapid method for REE and trace-element analysis using laser sampling ICP-MS on direct fusion whole-rock glasses. Chemical Geology, 106, 229–249.

Gao S., Liu X.M., Yuan H.L., Hattendorf B., Günther D., Chen L. and Hu S.H. (2002)
Determination of forty-two major and trace elements in USGS and NIST SRM glasses by laser ablation-inductively coupled plasma-mass spectrometry. Geostandards Newsletter: The Journal of Geostandards and Geoanalysis, 26, 181–196.

Gray A.L. (1985)
Solid sample introduction by laser ablation for inductively coupled plasma source-mass spectrometry. Analyst, 110, 551–556.

Guillong M. and Günther D. (2002)
Effect of particle size distribution on ICP-induced elemental fractionation in laser ablation-inductively coupled plasma-mass spectrometry. Journal of Analytical Atomic Spectrometry, 17, 831–837.

Guillong M., Hametner K., Reusser E., Wilson S.A. and Günther D. (2005)
Preliminary characterisation of new glass reference materials (GSA-1G, GSC-1G, GSD-1G and GSE-1G) by laser ablation-inductively coupled plasma-mass spectrometry using 193 nm, 213 nm and 266 nm wavelengths. Geostandards and Geoanalytical Research, 29, 315–331.

Günther D. and Hattendorf B. (2005)
Solid sample analysis using laser ablation inductively coupled plasma-mass spectrometry. Trends in Analytical Chemistry, 24, 255–265.

Halicz L. and Günther D. (2004)
Quantitative analysis of silicates using LA-ICP-MS with liquid calibration. Journal of Analytical Atomic Spectrometry, 19, 1539–1545.

He Y.S., Li S.G., Hoefs J., Huang F., Liu S.A. and Hou Z.H. (2011)
Post-collisional granitoids from the Dabie orogen: New evidence for partial melting of a thickened continental crust. Geochimica et Cosmochimica Acta, 75, 3815–3838.

Hu Z.C., Liu Y.S., Li M., Gao S. and Zhao L.S. (2009)
Results for rarely determined elements in MPI-DING, USGS and NIST SRM glasses using laser ablation ICP-MS. Geostandards and Geoanalytical Research, 33, 319–335.

Hu Z.C., Zhang W., Liu Y.S., Chen H.H., Gaschnig R.M., Zong K.Q., Li M., Gao S. and Hu S.H. (2013)
Rapid bulk rock decomposition by ammonium fluoride (NH_4F) in open vessels at an elevated digestion temperature. Chemical Geology, 355, 144–152.

Jarvis K.E. (1988)
Inductively coupled plasma-mass spectrometry: A new technique for the rapid or ultra-trace level determination of the rare-earth elements in geological materials. Chemical Geology, 68, 31–39.

Jarvis K.E. and Williams J.G. (1993)
Laser ablation inductively coupled plasma-mass spectrometry (LA-ICP-MS): A rapid technique for the direct, quantitative determination of major, trace and rare-earth elements in geological samples. Chemical Geology, 106, 251–262.

Jenner G.A., Longerich H.P., Jackson S.E. and Fryer B.J. (1990)
ICP-MS – A powerful tool for high-precision trace-element analysis in Earth sciences: Evidence from analysis of selected USGS reference samples. Chemical Geology, 83, 133–148.

references

Jochum K.P., Scholz D., Stoll B., Weis U., Wilson S.A., Yang Q.C., Schwalb A., Börner N., Jacob D.E. and Andreae M.O. (2012)
Accurate trace element analysis of speleothems and biogenic calcium carbonates by LA-ICP-MS. Chemical Geology, 318–319, 31–44.

Kent A.J.R. and Ungerer C.A.A. (2005)
Production of barium and light earth element oxides during LA-ICP-MS microanalysis. Journal of Analytical Atomic Spectrometry, 20, 1256–1262.

Kurosawa M., Shima K., Ishii S. and Sasa K. (2006)
Trace element analysis of fused whole-rock glasses by laser ablation-ICP-MS and PIXE. Geostandards and Geoanalytical Research, 30, 17–30.

Lee Y.L., Chang C.C. and Jiang S.J. (2003)
Laser ablation inductively coupled plasma-mass spectrometry for the determination of trace elements in soil. Spectrochimica Acta Part B, 58, 523–530.

Li M., Hu Z.C., Gao S. and Liu Y.S. (2011)
Direct quantitative determination of trace elements in fine-grained whole rocks by laser ablation-inductively coupled plasma-mass spectrometry. Geostandards and Geoanalytical Research, 35, 7–22.

Liu Y.S., Hu Z.C., Gao S., Günther D., Xu J., Gao C.G. and Chen H.H. (2008)
In situ analysis of major and trace elements of anhydrous minerals by LA-ICP-MS without applying an internal standard. Chemical Geology, 257, 34–43.

Luo Y., Gao S., Longerich H.P., Günther D., Wunderli S., Yuan H.L. and Liu X.M. (2007)
The uncertainty budget of the multi-element analysis of glasses using LA-ICP-MS. Journal of Analytical Atomic Spectrometry, 22, 122–130.

Malherbe J., Claverie F., Alvarez A., Fernandez B., Pereiro R. and Molloy J.L. (2013)
Elemental analyses of soil and sediment fused with lithium borate using isotope dilution laser ablation-inductively coupled plasma-mass spectrometry. Analytica Chimica Acta, 793, 72–78.

Mukherjee P.K., Khanna P.P. and Saini N.K. (2014)
Rapid determination of trace and ultra-trace level elements in diverse silicate rocks in pressed powder pellet targets by LA-ICP-MS using a matrix independent protocol. Geostandards and Geoanalytical Research, 38, 363–379.

Nehring F., Jacob D.E., Barth M.G. and Foley S.F. (2008)
Laser-ablation ICP-MS analysis of siliceous rock glasses fused on an iridium strip heater using MgO dilution. Microchimica Acta, 160, 153–163.

Nicholls I.A. (1974)
A direct fusion method of preparing silicate rock glasses for energy-dispersive electron microprobe analysis. Chemical Geology, 14, 151–157.

Nielsen S.G. and Lee C.T.A. (2013)
Determination of thallium in the USGS glass reference materials BIR-1G, BHVO-2G and BCR-2G and application to quantitative Tl concentrations by LA-ICP-MS. Geostandards and Geoanalytical Research, 37, 337–343.

Park C.S., Shin H.S., Oh H., Moon J.H., Cho H. and Cheong C.S. (2013)
Determination of trace elements in geological reference materials G-3, GSP-2 and SGD-1a by low-dilution glass bead digestion and ICP-MS. Geostandards and Geoanalytical Research, 37, 361–368.

Pearce N.J.G., Perkins W.T. and Fuge R. (1992)
Developments in the quantitative and semi quantitative determination of trace elements in carbonates by laser ablation inductively coupled plasma-mass spectrometry. Journal of Analytical Atomic Spectrometry, 7, 595–598.

Perkins W.T., Pearce N.J.G. and Jeffries T.E. (1993)
Laser ablation inductively coupled plasma-mass spectrometry: A new technique for the determination of trace and ultra-trace elements in silicates. Geochimica et Cosmochimica Acta, 57, 475–482.

Pretorius W., Weis D., Williams G., Hanano D., Kieffer B. and Scoates J. (2006)
Complete trace elemental characterisation of granitoid (USGS G-2, GSP-2) reference materials by high resolution inductively coupled plasma-mass spectrometry. Geostandards and Geoanalytical Research, 30, 39–54.

Reid J.E., Horn I., Longerich H.P., Forsythe L. and Jenner G.A. (1999)
Determination of Zr and Hf in a flux-free fusion of whole rock samples using laser ablation inductively coupled plasma-mass spectrometry (LA-ICP-MS) with isotope dilution calibration. Geostandards Newsletter: The Journal of Geostandards and Geoanalysis, 23, 149–155.

Stoll B., Jochum K.P., Herwig K., Amini M., Flanz M., Kreuzburg B., Kuzmin D., Willbold M. and Enzweiler J. (2008)
An automated iridium-strip heater for LA-ICP-MS bulk analysis of geological samples. Geostandards and Geoanalytical Research, 32, 5–26.

Sun S.S. and McDonough W.F. (1989)
Chemical and isotopic systematics of oceanic basalts: Implications for mantle composition and processes. In: Saunders A.D. and Norry M.J. (eds), Magmatism in the Ocean basins. Geological Society of London, Special Publication, 42, 313–345.

Sylvester P. (2001)
Trace element analysis of fused whole rock glasses by laser ablation ICP-MS. In: Sylvester P. (ed.), Laser-ablation-ICP-MS in the Earth sciences. Short Course Series, 29, Mineralogical Association of Canada (Ottawa), 147–162.

Van Heuzen A.A. and Morsink J.B.W. (1991)
Analysis of solids by laser ablation-inductively coupled plasma-mass spectrometry (LA-ICP-MS) – II. Matching with a pressed pellet. Spectrochimica Acta Part B, 46, 1819–1828.

references

Wilson S.A. (1998)
Data compilation for USGS reference material GSP-2, Granodiorite, Silver Plume, Colorado. U.S. Geological Survey Open-File Report.

Yu Z.S., Robinson P. and McGoldrick P. (2001)
An evaluation of methods for the chemical decomposition of geological materials for trace element determination using ICP-MS. Geostandards Newsletter: The Journal of Geostandards and Geoanalysis, 25, 199–217.

Yu Z.S., Norman M.D. and Robinson P. (2003)
Major and trace element analysis of silicate rocks by XRF and laser ablation ICP-MS using lithium borate fused glasses: Matrix effects, instrument response and results for international reference materials. Geostandards Newsletter: The Journal of Geostandards and Geoanalysis, 27, 67–89.

Zhang W., Hu Z.C., Liu Y.S., Chen L., Chen H.H., Li M., Zhao L.S., Hu S.H. and Gao S. (2012)
Reassessment of HF/HNO_3 decomposition capability in the high-pressure digestion of felsic rocks for multi-element determination by ICP-MS. Geostandards and Geoanalytical Research, 36, 271–289.

Zhu L.Y., Liu Y.S., Hu Z.C., Hu Q.H., Tong X.R., Zong K.Q., Chen H.H. and Gao S. (2013)
Simultaneous determination of major and trace elements in fused volcanic rock powders using a hermetic vessel heater and LA-ICP-MS. Geostandards and Geoanalytical Research, 37, 207–229.

Supporting information

The following supporting may be found in the online version of this article:

Table S1. Concentration data from a profile in the W-2 fused glass.

This material is available as part of the online article from: http://onlinelibrary.wiley.com/doi/10.1111/j.1751-908X.2015.00352.x/abstract (This link will take you to the article abstract).